Multiphoton photoemission from laser-irradiated alpha -SiO_2

1993 J. Phys.: Condens. Matter 5 7033

(http://iopscience.iop.org/0953-8984/5/37/021)

J. Phys.: Condens. Matter 5 (1993) 7033–7046. Printed in the UK

Multiphoton photoemission from laser-irradiated α-SiO_2

Stephane Guizard, Philippe Martin and Guillaume Petite

Service de Recherche sur les Surfaces et l'Irradiation de la Matière, Commissariat à l'Energie Atomique, DSM/DRECAM, CE Saclay, 91191, Gif-sur-Yvette, France

Received 9 February 1993, in final form 27 April 1993

Abstract. Multiphoton photoemission of laser irradiated α-SiO_2 is studied as a function of different laser parameters. The laser is a frequency-doubled or -tripled Nd-YAG laser, operated in the picosecond pulse duration regime. The sample is a single crystal, cut perpendicularly to the C-axis direction, kept under ultra-high vacuum (UHV) conditions. The intensity dependence of the photocurrent reveals that emission at the second harmonic frequency is throughout the whole accessible intensity range governed by defect states, whereas at the third harmonic frequency we observe a transition from a two- to three-photon dynamics, which could reveal the onset of the valence band emission. However, the most probable explanation is still in both cases a two-photon, defect-driven, process, eventually followed by electron heating in the conduction band through electron–photon–phonon collisions, or by photon absorption by electrons trapped in the bottom of the conduction band. The dependence of the photocurrent from the laser polarization direction is shown to differ depending on whether all the emitted electrons are collected or only the ones emitted along the C-axis. In this last case, a selection rule seems to apply to the emission process that yields information about the symmetry of the emitting state.

1. Introduction

Photoemission from laser-irradiated solids is known to occur even when the photon energy is smaller than the work function of the solid, because of the laser ability, due to the high intensities delivered, to cause multiphoton transitions (that is involving the simultaneous absorption of several photons). In principle there is no other limit to the number of photons that can be absorbed in such a process than the laser intensity which can be effectively used in the experiment. This intensity is, in the case of solid targets, limited to the damage threshold of the material. In the case of wide-bandgap insulators, which essentially show no linear absorption, this threshold is rather high (in the GW cm^{-2} range, for usual nanosecond laser pulses) and can be further increased by reducing the laser pulse duration because it is the total energy absorbed that matters, whereas the instantaneous intensity is the parameter relevant to the appearance of a high-order multiphoton process.

Because of the important role played by wide-bandgap insulators as optical materials, their interaction with intense laser radiation has been studied to a certain extent, but mostly in the case of alkali and alkaline earths halides. One of the issues in such experiments was to decide whether the avalanche breakdown mechanism first proposed by Yablonovitch and Bloembergen (1972) would apply to such materials. Experimental investigations of this problem by Jones *et al* (1989) led these authors to propose an alternative model: by measuring the photoacoustic signal and the self-trapped exciton (STE) recombination luminescence as a function of laser intensity in several wide-bandgap materials, they were able to measure the energy transferred to the lattice at intensities below the damage threshold. These measurements have shown that multiphoton processes may be efficient in generating

0953-8984/93/377033+14$07.50

a high density of free carriers even when absorption of four or five photons is necessary to bridge the band-gap. More importantly, they proved that an important heating of the lattice occurs during the laser pulse, which increases non-linearly with laser intensity. This local heating due to electron–photon–phonon collisions may increase the temperature up to the melting point, thus inducing the damage.

In this context, multiphonon photoemission (MPE) can yield important and specific information: not only are the transitions involved in this process the same as those that cause (multiphonon) carrier photoinjection, but MPE is at the origin of a wide variety of spectroscopic methods which were proved fruitful in the gas phase, as in the case of metallic samples (Steinman 1989), and could also be applied to the case of insulators, provided that specific difficulties that pertain to photoelectron spectroscopy in insulators are solved. In this paper, we do not intend to go that far, but only to show that the measurement of the total photocurrent in laser irradiation of wide-bandgap oxides can yield valuable information on the processes at work in such interactions. The experiments reported here were carried on α-SiO_2 because among the wide-bandgap oxides currently used as optical materials, it is the one for which most structural information (including to a certain extent the valence and conduction band structure) are available. It is also worth noting that complementary experiments were performed on the trapping (through excitonic mechanisms) of electronic excitations in this material (Joosen *et al* 1992).

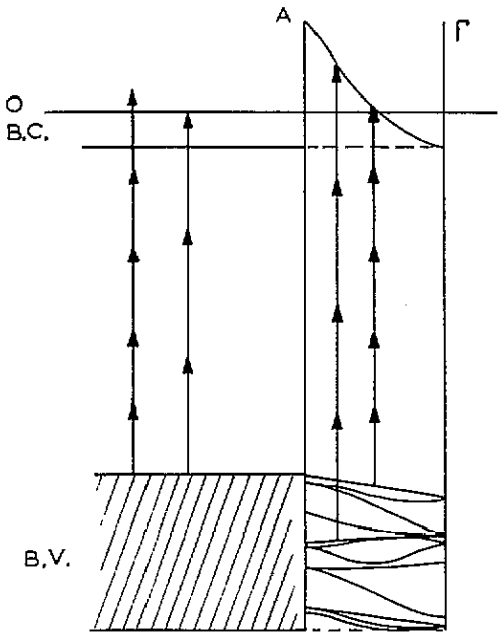

Figure 1. Multiphoton interband transitions in α-SiO_2. On the left part of the figure all lowest order (direct and indirect) transitions are considered. The right part of the figure shows direct transitions in the ΓA direction (normal to the sample surface), the band structure is taken from Chelikowsky and Schlüter (1977). (B.V.: valence band, B.C.: conduction band).

2. The general framework: multiphoton processes

The principle of a multiphonon photoemission process is represented in figure 1, where

the band structure is that of α-SiO_2 in the ΓA direction (corresponding to emission along the C-axis), and only direct processes are considered. The band structure is taken from Chelikowsky and Schlüter (1977). Note that for a 3.51 eV photon energy (one of the energies in this experiment), no direct three-photon interband transition is possible, whereas a three-photon indirect transition leads to injection of an electron right at the vacuum level. Independent of the specifics of the band structure, an important aspect in the case of wide-bandgap systems at visible wavelengths is that there is no energy-conserving interband transition that can provide resonant intermediate states in the MPE process. This situation is opposite to that encountered, for instance, in metals (see Martin *et al* (1992) and references therein). However, it has been clearly proven in the case of atoms that this does not prevent multiphoton absorption to occur (see Agostini and Petite 1988): the processes depicted in figure 1 are typical cases of five- and three-photon non-resonant transitions which are necessary to excite an electron from the valence to the conduction band using, respectively, 2.34 eV and 3.51 eV photons. If the vacuum level is below the energy reached in the conduction band, the electron can escape from the sample and cause photoemission. Non-resonant multiphoton processes require high intensities because simultaneous absorption of several photons is a prerequisite, since the lifetime of non-resonant (virtual, that is non-energy-conserving) intermediate states is limited by the Heisenberg principle to a time of the order of the laser period.

The general theory accounting for such processes, in the intensity range considered in this paper, is lowest (non-vanishing) order perturbation theory. In essence, it is not necessary, as long as the laser field does not approach the binding field of the electron, to go beyond the nth order of perturbation theory for a n-photon process. This allows one to express the number of electrons N_c injected into the conduction band by a laser pulse of duration τ and intensity I as:

$$N_c = N_v \sigma_n \tau_n F^n \tag{1}$$

where N_v is the number of valence electrons which can be excited, σ_n is an intensity-independent parameter known as the generalized cross section (in cm^{2n} $s^{(n-1)}$), τ_n an effective interaction time (in the case of a Gaussian pulse $\tau_n = \tau/\sqrt{n}$), and F the photon flux, with the units chosen here. If one assumes that the escape probability of a conduction electron above the vacuum level is not a function of the free-carrier density, the photocurrent will follow an intensity dependence similar to (1). Measuring the intensity dependence of the photocurrent thus yields the number of photons absorbed in the process. The usual representation used log–log coordinates and the slope of the straight line representing the behaviour of (1), that is the order of non-linearity of the process, is the number of photons absorbed.

3. Experimental setup

The experiment consists in a laser system whose output beam is focused onto a sample, kept under ultra-high vacuum (UHV) conditions, in front of a time-of-flight ion mass/electron energy spectrometer. The details of this setup are thoroughly explained in Martin *et al* (1992), and we restrict ourselves here to a reminder of the main characteristics of this apparatus.

The laser is a Nd:YAG oscillator/amplifier system (figure 2) operated in the picosecond regime. It delivers, at a 20 Hz repetition rate, pulses with a duration between 35 and 150 ps

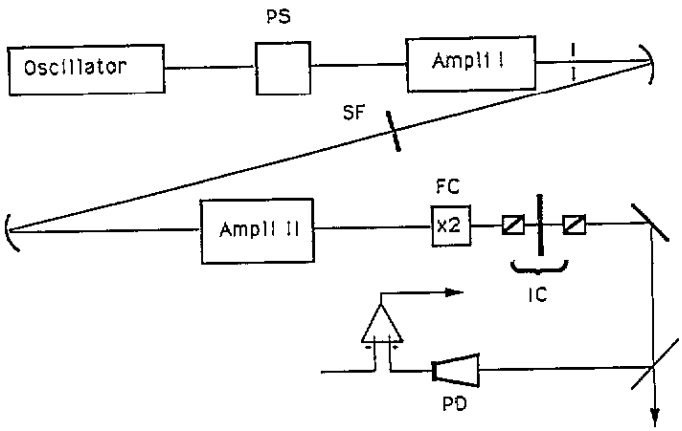

Figure 2. Outline of the laser system. PS: pulse selector, SF: spatial filter, FC: frequency conversion, IC: intensity control and PD: photodiode.

(29 and 95 ps) at the second (third) harmonic frequency, that is at a photon energy of 2.34 eV (3.51 eV). The pulse-to-pulse intensity fluctuations are less than ±5%, which is also the limits within which is contained the long-term intensity drift. Before focusing in the experiment, the beam is spatially filtered in order to obtain a diffraction-limited beam. An intensity of up to 100 GW cm^{-2} can be reached on the sample, this being close to the damage threshold for this pulse duration. Note that all intensities quoted hereafter are measured in a cross-section of the beam. Intensities along the surface must take into account the large incidence angle (75°), and are therefore reduced. However, the relevant physical parameter in this experiment is the electric field of the laser, which is linked to the cross-sectional intensity used here.

The sample and the detection apparatus are placed in a UHV chamber, where the pressure is kept below 10^{-10} Torr. The sample is an α-quartz single crystal cut perpendicularly to its optical axis (or C-axis). Its surface is prepared by baking at 950° in the air, in order to preserve surface stoichiometry. Surface ordering was checked using low energy electron diffraction (LEED). In the case of insulating samples, charging effects can affect the diffraction patterns. However, it is known that the changes in the surface potential due to such charging saturates at a finite value (of the order of a few volts), so that LEED patterns can be obtained provided one works at an electron energy somewhat higher than usual (around 110 eV). The detector consists in a time-of-flight spectrometer which can be used in two alternate configurations (see figure 3). Electrons are collected by setting the spectrometer at a positive voltage, and all elements in the electrostatic reflector at the same potential as the flight tube. If this potential is high (typically 2 kV), all the emitted electrons are collected, but the energy resolution is lost. If this potential is low (typically 5 V), an energy resolution of 0.1 eV can be obtained, but the collection efficiency is low: only the electrons emitted towards the detector (that is with momentum aligned along the ΓA direction) are collected. Total photocurrent measurements were also made in a separate experiment where the sample was placed directly in front of an electron multiplier. The results obtained in this way simply confirmed those obtained with the time-of-flight spectrometer set at a high potential.

Positive ions are collected setting the flight tube at a high negative voltage and the electrostatic reflector in action. In this configuration, known as the 'reflectron mode', a mass spectrum of the positively charged emitted species is obtained. Inverting the polarity

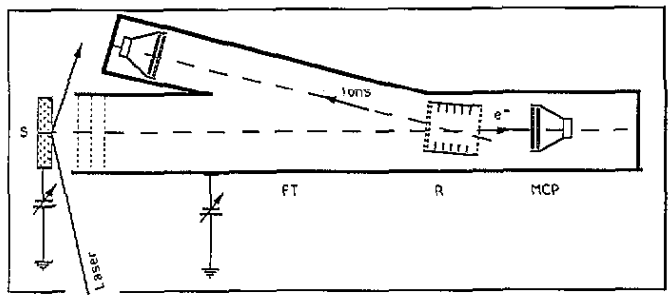

Figure 3. Electron energy/ion mass spectrometer. S: sample, FT: flight tube, R: electrostatic reflector and MCP: michrochannel plate.

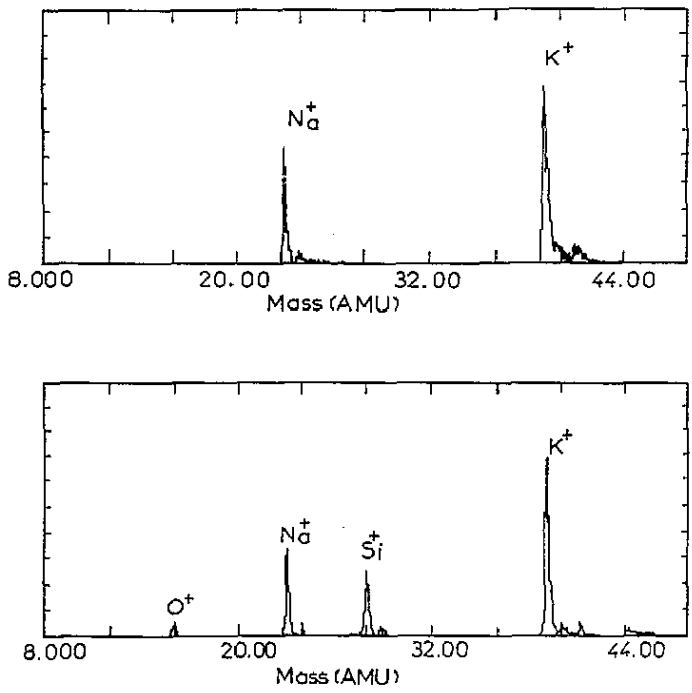

Figure 4. Ion-mass spectra obtained for two different laser intensities (E_p = 2.34 eV). Top: I = 800 MW cm^{-2}, only alkali ions are desorbed. Bottom: I = 20 GW cm^{-2}, shows the onset of Si and O emission.

of the system allows detection of negative ions. Such ion mass spectra were used to check the surface purity, and set an upper limit to the intensity to be used in the experiment. Two ion mass spectra corresponding to two different laser intensities are shown in figure 4. On the first one, for a laser intensity of 0.8 GW cm^{-2}, only alkali ions (essentially Na and K) can be detected. This signal can never completely be suppressed, probably because of the relative ease with which alkalis are laser desorbed, and also because of the fact that alkali ions migrate preferentially along the 'channels' parallel to the optical axis. This migration, under a high DC voltage, can in principle be used to purify the sample ('sweeping'), but even this method did not succeed in totally suppressing the alkali signal. When the intensity is increased, this alkali signal saturates, and Si^+ and O^+ ions can be detected. At this point,

it is clear that laser etching of the sample begins. One should however keep in mind that the spectra of figure 4 correspond to the emission of a few ions from an area of at least 10^{-5} cm^2 (and often much more), which is still negligible. This is also a probable reason for the persistence of the alkali ion signal. Any increase of the intensity from this point on leads to a rapid increase of the Si^+ and O^+ ion signal, leading to a situation where macroscopic laser ablation of the sample surface is obvious. In such a case, the resolution of the mass spectrometer is drastically reduced, most probably because many ions leave the surface as clusters which dissociate later on (neutral species can then be detected on the electron detector), a situation where our collection setup is inadequate. In both cases (electron and ion emission), the detector output is fed to a 350 MHz bandwidth storage oscilloscope and processed numerically with the help of a microcomputer.

An obvious question is to what extent are our photocurrent measurements perturbed by the positive charge left behind by the electrons leaving the sample. Two different answers can be given, depending on whether we consider the problem of one single pulse, or that of an average charge resulting from the accumulation of several hundreds of laser shots. Let us consider the problem of a single pulse first. This situation is common to all such experiments and is known to result, in the 'space charge' regime, in saturation of the photocurrent when the intensity is increased beyond a certain level (Martin *et al* 1992, Petite *et al* 1992). Such effects were apparent in our experiment, as shown hereafter. Another problem is that of the accumulation of a positive charge on the sample resulting from a large number of laser shots. As will be reported in detail elsewhere, this problem can be circumvented by heating the sample at a temperature of about 350 °C or above. Without entering into too much detail, this allows thermal detrapping of the charges, that is a thermally induced conductivity, which yields two different effects: (i) on the total photocurrent, which increases by more than one order of magnitude when the temperature is increased from room temperature to 350 °C, (ii) on the photoelectron spectrum which shifts towards low energies (down to seemingly 'negative' energies) for a room temperature sample, and is on the contrary stable when the sample is heated (Petite *et al* 1985). The stability of the photoelectron spectrum is an unambiguous sign that no progressive charging of the sample occurs when the sample is heated, and all experiments reported hereafter have thus been performed at sample temperatures of 350°C or above.

4. Experimental results

4.1. Intensity dependence

Figures 5 and 6 present the results of two experiments using respectively the second (E_p = 2.34 eV) and the third (E_p = 3.51 eV) harmonics of our laser. As shown by the excitation diagrams of figure 1, one expects in this case that emission will require respectively $n = 5$ and 3 (four for direct transitions) photons for a valence band electron, and thus an experimental order of non-linearity K equal to such values of n.

The experimental order of non-linearity that can be measured from the plot of figure 5 is equal to 2.3. The experiment was repeated in a large variety of situations, leading to the conclusion that the order of non-linearity is always much lower than 5, that is $2 < K < 3$. On the upper part of the curve, an inflexion of the curve is clearly seen, which is due to an experimental saturation, most likely because of space charge. In the case of figure 5, the laser was not tightly focused on the sample, and the intensity is very low (in the 10 MW cm^{-2} range). The experiment was also performed with a focused laser, at an intensity in the GW cm^{-2} range, leading to the same result.

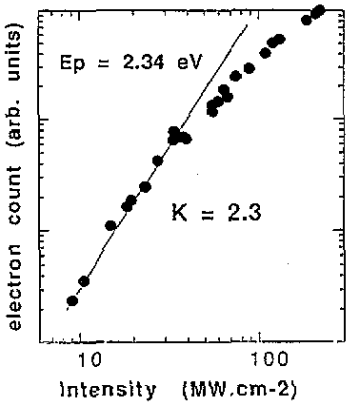

Figure 5. Intensity dependence of the MPE current for $E_p = 2.34$ eV (average photocurrent: approx. 10^4 e^- cm^{-2} per laser shot).

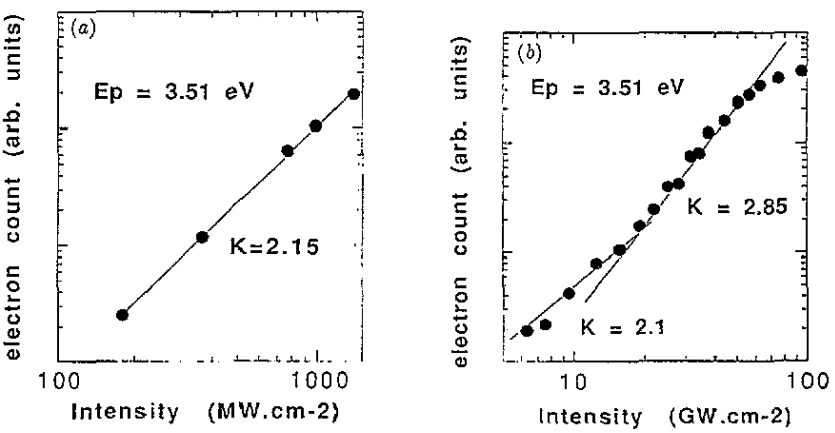

Figure 6. Intensity dependence of the MPE current for $E_p = 3.51$ eV. Two different experimental configurations have been used, giving access to two different intensity ranges. (*a*) unfocused beam (average photocurrent: approx 10^4 e^- cm^{-2} per laser shot), (*b*) focused beam (average photocurrent: approx. 10^7 e^- cm^{-2} per laser shot).

On figure 6 ($E_p = 3.51$ eV), where a three-photon process is expected, the situation is somewhat different. With a mildly focused laser, at intensities in the 10 MW cm^{-2} range, the same result as with the second harmonic is observed (figure 6(*a*)), that is a low order of non-linearity. When the laser is tightly focused, so that intensities in the 10 GW cm^{-2} range are used (that is just below the damage threshold), a change in the dynamics of the emission process is seen (figure 6(*b*)). The lower part of the curve seems to reproduce the result of figure 6(*a*), but increasing the intensity leads into a regime where the order of non-linearity is close to three. The overall result suggests a transition from a two-photon to a three-photon regime at intensities around GW cm^{-2}.

4.2. Angular dependence

In another experiment, the intensity is kept constant, but the angle of polarization of the laser electric field (which is linearly polarized) with respect to the surface is varied. This was done for two different collection configurations. In the case of figure 7, the total

photocurrent was collected. In such an experiment on metallic samples, it is usually found that the signal is maximum when the laser is p-polarized (perpendicularly to the sample surface). There are two reasons for this behaviour: first, surface photoemission is strictly forbidden for s-polarization (because of the translational invariance of the surface potential); second, because in the case of bulk emission, one expects the electrons to be accelerated mainly along the laser polarization direction. In this experiment, the counter-intuitive result is obtained that about ten times more electrons are extracted from the sample with an s-polarization than with a p-polarization. As shown on figure 8, a completely different result is obtained when only the electrons propagating perpendicularly to the sample are detected. In this case, a few more electrons are collected in the case of a p-polarized laser than with an s-polarized one. The result of figure 8 was obtained with a flight tube set at a 20 V potential. In this case the half angle of collection for electrons leaving the surface with a kinetic energy of 1 eV is of 6° 30′.

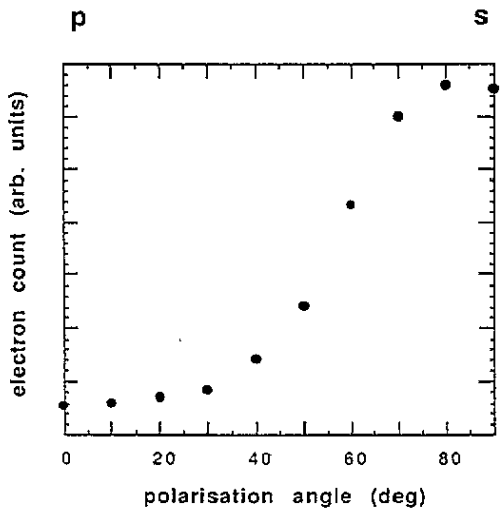

Figure 7. Dependence of the total MPE current on the laser polarization angle.

5. Discussion

Let us first summarize the results presented in the preceding section. Orders of non-linearity obtained for the intensity dependence of the photocurrent are generally lower than expected ($2 < K < 3$ at 2.34 eV instead of 5 as expected, 2 at 3.51 eV instead of 3 as expected), sometimes fractional (at 2.34 eV). When the intensity is increased, an increase of the order of non-linearity up to the expected value can be observed at 3.51 eV. Also note that the current is detected at quite low intensities (in the 10 MW cm^{-2} range). The dependence of the photocurrent on the laser polarization angle differs according to the collection geometry. When the total current is detected, s-polarization seems about ten times more efficient than the p-polarization. On the contrary, when only the electrons emitted in a small angle around the normal to the surface are collected, p-polarization is more efficient.

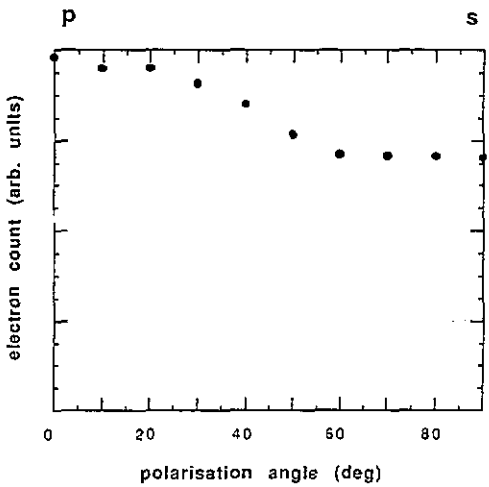

Figure 8. Dependence of the MPE current emitted in a 6° 30′ half-angle around the normal to the sample on the laser polarization angle.

There is a seemingly obvious explanation for the low orders of non-linearity observed at low intensities: assuming that it represents the number of photon absorbed, we conclude that emission does not arise from the excitation of valence band electrons, but instead from states in the bandgap, that is from defect states. Such defect states can originate from impurities, structural defects (eventually laser induced laser defects).

Concerning the impurities, the alkali seems the only possible candidate. However, we checked that the total electron current was orders of magnitude larger than the total alkali-ion current. We also verified that the intensity threshold for electron emission was more than one order of magnitude smaller than the one for ion emission. If we add to these observations the fact that the collection potential used for electron detection tends to sweep the alkali ions away from the sample surface, contrary to what happens in the positive ion detection configuration, it seems safe to assume that the alkali ions are not responsible for the electron emission.

Structural defects seem a much better choice for the origin of the defect states involved in the emission process. In particular, the E' centre (an unpaired electron located on an oxygen vacancy) has all the necessary features: it is known to have an optical absorption band beginning at 5 eV, which locates this state around 6 eV below the vacuum level. This would correspond to a three-photon absorption process at 2.34 eV, and a two-photon absorption process at 3.51 eV, in reasonable agreement with our observations. Moreover, E' centres in quartz are known to result from the relaxation of self-trapped excitons (STE) when the temperature exceeds 140 K (Tsaï and Griscom 1991, and references therein), and STE are a known product of sub-bandgap laser irradiation in quartz as well as in ionic crystals (Williams and Song 1990, Joosen *et al* 1992).

Whatever the nature of the defects which are at the origin of the measured emission, we can obtain an order of magnitude of the defect density needed to overcome the valence band emission. For this we use a scaling law for the generalized cross section in equation (1), which is generally admitted in the gas phase, and was also proven to be right in the case

of wide-bandgap insulators (Shen *et al* 1987, Jones *et al* 1989):

$$\sigma_n = 10^{19} x [10^{31}]^{(n-1)} \qquad (\mathrm{cm}^{2n}\ \mathrm{s}^{(n-1)}) \tag{2}$$

which allows one to compute within one order of magnitude a usual nth order 'generalized' cross-section. Using such orders of magnitudes, and a Gaussian shape assumption for τ_n, one obtains for the transition probabilities in our experimental conditions for two-, three- or five-photon processes the values in table 1 (at 2.34 eV) and table 2 (at 3.51 eV), at two different laser intensities.

Table 1. Multiphoton transition probabilities for three- and five-photon absorption processes, at a 3.51 eV photon energy, and intensities of 10 MW cm^{-2} and 10 GW cm^{-2}.

I (W cm^{-2})	n	$\sigma_n F^n \tau_n$
10^7	3	4×10^{-16}
	5	2×10^{-27}
10^{10}	3	4×10^{-7}
	5	2×10^{-12}

Table 2. Multiphoton transition probabilities for two- and three-photon absorption processes, at a 3.51 eV photon energy, and intensities of 10 MW cm^{-2} and 10 GW cm^{-2}.

I (W cm^{-2})	n	$\sigma_n F^n \tau_n$
10^7	2	7×10^{-11}
	3	1×10^{-16}
10^{10}	2	7×10^{-5}
	3	1×10^{-7}

Two conclusions can be derived from the comparison of the results in the third column of these two tables: let us consider the case of a photon energy of 2.34 eV. At 10 MW cm^{-2}, it takes about 10^{27} 'active' electrons to obtain one photoemission event. If we assume a valence band emission, we have to consider the electrons occupying the top of the valence band only (O_{2p} non-bonding orbitals). Our detection threshold is of the order of 0.1 electron per laser shot, so that we arrive at the conclusion that it would require an emitting volume of the order of 10^4 cm^3. In the unfocused geometry, the irradiated surface on the sample is of the order of 10^{-2} cm^2. Assuming a 10 nm escape depth for the electrons yields an emitting volume of the order of 10^{-8} cm^3. The assumption of a valence band emission thus seems unrealistic (by large enough that even an uncertainty of a few orders of magnitude on the generalized cross sections would not modify this conclusion). This gives more convincing evidence for a defect-dominated emission process.

Another conclusion derives from the comparison of the emission probabilities at 10 GW cm^{-2}, which is that a defect concentration of the order of 1 ppm is enough to ensure that, even in the high-intensity regime, the signal is dominated by defect emission (remember that not all electrons are 'active' for the MPE process, but only the top-most in the valence band). This defect concentration seems quite reasonable in view of other measurements of laser induced defect densities which, under intense irradiation yield figures in the 10^{17} cm^{-3} range (for instance see Devine 1989 or Tsaï *et al* 1988). However, at such concentrations, a three-photon process seems unable to account for the observation of

a signal at a 10 MW cm^{-2} intensity. We leave this point aside for a moment and turn to the situation at 3.51 eV.

As shown in figure 1, the number of photons necessary to produce an interband transition depends on whether indirect transitions are considered. Because of the extreme sensitivity of the probability to the number of photons absorbed, and also because no angular selection was used in this experiment (except in one case specified below), we will consider that the lowest order process (three-photon indirect transition) is the most probable one, and base our discussion on it.

As already noted, even a three-photon cross-section seems too small to account for a valence band emission at 10 MW cm^{-2}. A two-photon, defect driven, process yields a much more comfortable solution: assuming a defect density of 10^{18} cm^{-3}, and a 10^{-8} cm^3 emitting volume yields a high enough electron count at 10 MW cm^{-2}, in good agreement with the measured order of non-linearity. At 10 GW cm^{-2}, on the other hand, it is quite reasonable to expect the three-photon process to begin to dominate. A reasonable interpretation of the results at 3.51 eV then would be that at low intensities only the defect emission is observed, and, at high intensities, overcomed by the valence band emission whose probability grows faster with the laser intensity than the defect emission. The same argument applied to the case of 2.34 eV, taking into account the larger unbalance between defect and valence-band emission, explains why the latter is never observed. However, we have already noted that assuming a three-photon defect emission does not yield, at a 2.34 eV photon energy, reasonable figures. Of course, if the defect emission was also a two-photon process at 2.34 eV, the order of magnitude of the probabilities would be, as for 3.51 eV, more reasonable. It would then be necessary to understand why the intensity dependence at 2.34 eV yields an experimental order of non-linearity higher than two (a lowering of this experimental order of non-linearity due the transport of the electrons to the surface is much easier to admit). As we have seen, it cannot be because of the onset of valence band emission. Note that not only the orders of magnitude of the probabilities (after all computed using an approximate scaling law) precludes this possibility, but also the fact that, because a five-photon process has an extremely steep intensity dependence, it would cause abrupt changes in the experimental order of non-linearity as soon as it starts to dominate, which is clearly not observed.

There is, however, another interpretation which is suggested by the observation of Shen *et al* (1987) concerning the laser heating of electrons in the conduction band of different insulators, including SiO_2. The basic physical process involved in such a heating is a three-body electron–photon–phonon collision. Only in such a collision can a conduction electron absorb energy from the EM field conserving both the total energy and the total momentum. Such collisions have been introduced in a recent Monte Carlo calculation by Cartier and Arnold (1993), and were shown to occur at a rate of about 2×10^{12} s^{-1}, at an intensity of 1 TW cm^{-2}, and a photon energy of 4.5 eV. This rate certainly increases when the photon energy is smaller, but it also increases linearly with the laser intensity, so that it is most likely high enough to make such a collision very probable in a 35 ps laser pulse with peak intensities in the GW cm^{-2} range. Of course, this probability becomes very small at 10 MW cm^{-2}, but the state-of-the-art concerning the description of the SiO_2 conduction band, and thus of the phonon structure, is too embryonic to rule out this possibility. It seems to us the best possible explanation for the results of this photoemission experiment, because it would explain simultaneously the results obtained at 2.34 eV and 3.51 eV. If this is the case, it is not certain at all that the three-photon process that we observe at 3.15 eV is the valence band emission. It could also be, as in the case of 2.34 eV, a sequential process involving one two-photon absorption by a defect state and one electron–photon–phonon

interaction in which one photon is absorbed. The probability of such sequential processes still increases if one takes into account the possibility that the electron, after relaxation through electron–phonon collisions (an extremely fast process: picosecond time scale) in the bottom of the conduction band, becomes trapped there through its interaction with the ion lattice (small polaron model, see Blaise (1992) and references therein). Such states have a very long lifetime compared to the laser pulse duration, and a potential is provided through the lattice polarization that makes photon absorption possible. Figure 9 finally shows a pictorial representation of what we believe is the most probable interpretation of our results. In such a case, the defect state involved would be located between 3.51 and 4.68 eV below the vacuum level, which means that it would probably not be due to an E' centre.

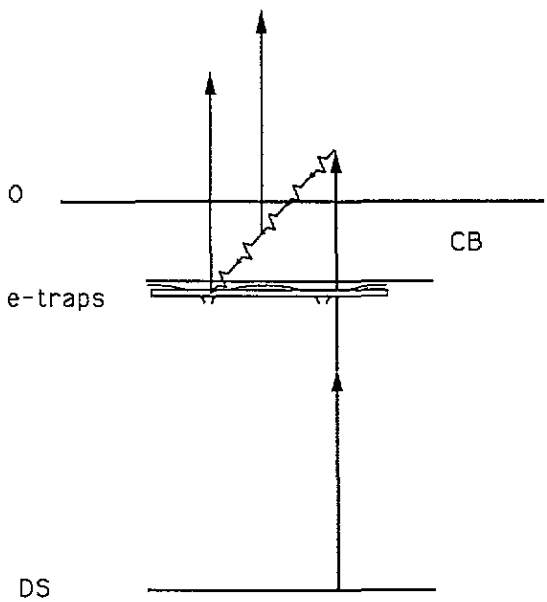

Figure 9. Schematic representation of a defect-driven emission process including electron heating in the conduction band through electron–photon–phonon collisions and absorption by electrons trapped in the bottom of the conduction band. DS: defect state, CB: conduction band and 0: vacuum limit.

A question then arises concerning the additional experiments that would help checking this interpretation. Clearly, a measure of the photoelectron energy spectrum in such emission processes would be an extremely valuable source of information. However, in the case of insulating samples, such photoelectron energy spectra are difficult to interpret, but an experimental effort in this direction is certainly the next step in these experiments.

Let us turn now to the results concerning the polarization dependence of the photocurrent which are intriguing in two respects. Firstly, because, concerning the total photocurrent (no angular resolution), a counterintuitive result is obtained. Two remarks come to mind concerning this observation: first that the emission could essentially depend on the angle between the laser polarization and the crystal main directions. Such an idea should be checked by using samples with different crystallographic orientations, and eventually rotating the crystal around the normal to its surface. This dependence should also be investigated for an amorphous sample. The second remark is that if, as suggested above,

electron–phonon collisions play an important role in the emission process, the momentum of the outgoing electron may be essentially supplied by the phonons (electron–phonon collisions are known to be large angle scattering events).

A second observation is the difference between the results obtained when an angularly selective detection system is used. Comparison of figures 7 and 8 suggest that emission normally to the surface is reduced (forbidden?) when the laser polarization is parallel to the surface. This could be understood in the general framework of angle-resolved photoemission experiments as a result of a selection rule concerning our MPE process. In such an experiment (angle-resolved photoemission perpendicular to the surface), the general rule is that the final state in the optical transition that causes emission should be invariant under all the operations of the semi-infinite crystal symmetry group (see for instance Spanjaard and Desjonqueres (1993)). It is then possible to obtain information about the symmetry of the initial state using the fact that for a given laser polarization the multiphonon matrix element of interest vanishes. The results of figures 7 and 8 are still preliminary but we think they provide a good demonstration of the potential of such measurements in MPE studies.

6. Conclusion

We have investigated the multiphoton photoemission of α-SiO_2 under intense laser irradiation by visible light (2.34 eV and 3.51 eV) in the picosecond regime, for an intensity range up to the ablation threshold. We have obtained evidence that, despite the use of high purity samples, the emission is still generally a defect-driven process. To account for the dynamics of the MPE process, it is necessary to include the effect of laser heating of the electrons in the conduction band, either through electron–photon–phonon collisions or through photoabsorption by trapped electrons. These effects are more likely to explain the observation of changes in the experimental order of non-linearity than the onset of a valence band emission, even if in the case where few (three) photons are necessary for this emission, it cannot be excluded. Photoelectron energy spectroscopy should allow one to decide between these different possibilities. The polarization dependence of the photocurrent shows unusual behaviour which could be due to the influence of the crystalline structure, but also to the effect of electron–phonon collisions. A detailed study of these effects may bring about some important observations concerning the symmetry of the states involved in the emission process.

Acknowledgments

The authors wish to thank G Blaise, M C Desjonquères, J P Duraud, F Jollet, W Joosen and D Spanjaard for many fruitful discussions, and F Bart and L Douillard for their help with the sample preparation. They also want to thank C Le Gressus and C Boiziau for their constant interest in this work. Technical assistance from E Caprin was extremely valuable.

References

Agostini P and Petite G 1988 *Contemp. Phys.* **29** 57

Arnold D and Cartier E 1992 *Phys. Rev.* B **46** 15 102

Blaise G 1992 *Dielectrics: Proc. Interdisciplinary Conf. on Dielectrics (Antibes-Juan les Pins, 1992)* (Paris: SFV) pp 1, 27

Chelikowsky J R and Schlüter M 1977 *Phys. Rev.* B **15** 4020
Devine R 1989 *Phys. Rev. Lett.* **62** 340
Jones S C Braunlich P, Casper R T, Shen X A and Kelly P 1989 *Opt. Eng.* **28** 1039
Joosen W, Guizard S, Martin P, Petite G, Agostini P, Dos Santos A, Grillon G, Hulin D, Migus A and Antonetti A 1992 *Appl. Phys. Lett.* **61** 2260
Martin P, Trainham R, Agostini P and Petite G 1992 *Phys. Rev.* B **45** 69
Petite G, Agostini P, Boiziau C, Vigouroux J P, Le Gressus C and Duraud J P 1985 *Opt. Commun.* **53** 189
Petite G, Agostini P, Trainham R, Mevel E and Martin P 1992 *Phys. Rev.* B **45** 12210
Shen X A, Jones S C, Braunlich P and Kelly P 1987 *Phys. Rev.* B **36** 2831
Spanjaard D and Desjonqueres M C 1993 *Concepts in Surface Science (Springer Surface Science Series)* (New York: Springer) at press
Steinman W 1989 *Appl. Phys.* A **49** 365
Tsaï T E and Griscom D L 1991 *Phys. Rev. Lett.* **67** 2517
Tsaï T E, Griscom D L and Friebele E J 1988 *Phys. Rev. Lett.* **61** 444
Williams R T and Song K S 1990 *J. Phys. Chem. Solids* **51** 679
Yoblonovitch E and Bloembergen N 1972 *Phys. Rev. Lett.* **29** 907